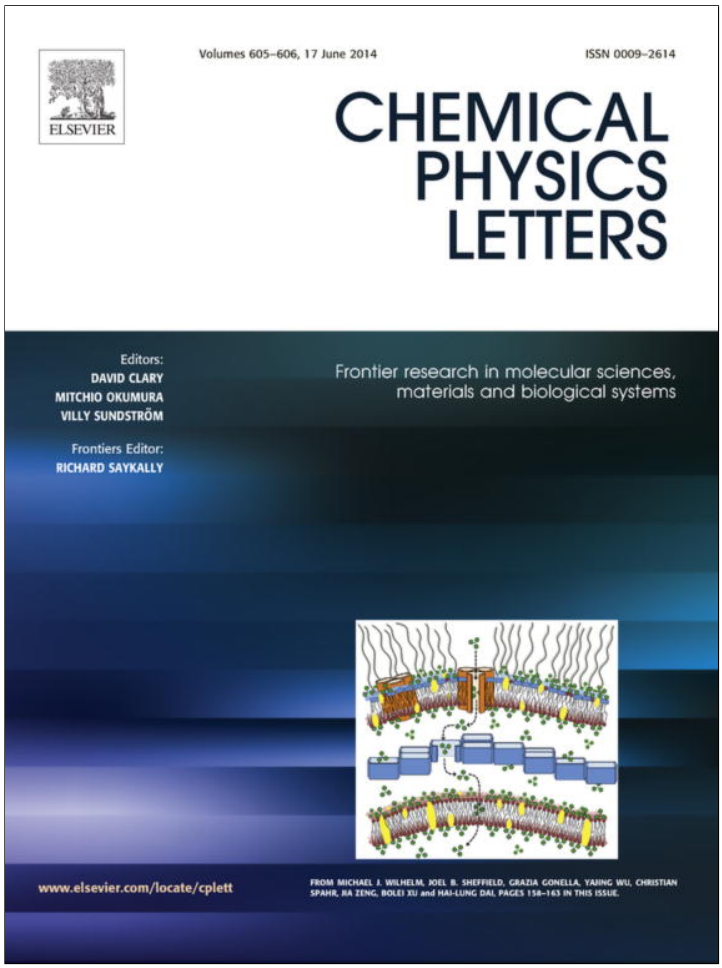

Chemical Physics Letters 605–606 (2014) 137–146

Contents lists available at ScienceDirect

Chemical Physics Letters

journal homepage: www.elsevier.com/locate/cplett

Generalized interatomic pair-potential function

Jianing Colin Xie [a,b], Sudhanshu K. Mishra [c], Tapas Kar [a,*], Rui-Hua Xie [d,e,*]

[a] Department of Chemistry and Biochemistry, Utah State University, Logan, UT 84322, USA
[b] A&M Consolidated High School, College Station, TX 77840, USA
[c] Department of Economics, North-Eastern Hill University, Shillong 793022, India
[d] Department of Applied Physics, Xi'an Jiaotong University, Xi'an 710049, China
[e] Department of Physics, Hubei University, Wuhan 430062, China

ARTICLE INFO

Article history:
Received 17 April 2014
In final form 11 May 2014
Available online 20 May 2014

ABSTRACT

Based on a three-parameter molecular orbital-type pair-potential function, we have proposed a generalized interatomic pair-potential function. This new function has been demonstrated to be able to describe accurately and adequately the potentials of the metastable diatomic dications (e.g., He_2^{++}, BeH^{++}, AlH^{++}), and the ground states of covalent bonding systems (e.g., H_2, Si_2, HCl, NO, LiH, HeH^+, and He_2^+), ionic bonding systems (e.g., NaCl), and van der Waals weakly binding systems (e.g., rare-gas, alkaline-earth, group 12, rare-gas metal dimers, and rare-gas halides).

1. Introduction

The nature of interatomic potentials [1–6] determines the static and dynamical properties of matter in solid, liquid and gas phases, such as equilibrium geometry [2], threshold displacement energy [5], chemical-reaction mechanism [4], heat conductivity [2], transport coefficients [3], stability of biologic compounds DNA and RNA [2], and high-density energy storage materials [6]. Further, in many areas today, computer simulations [2–4] are becoming an integral part of many research investigations and provide help in understanding various problems at atomistic levels, for example, exploring macroscopic properties of gases under extreme conditions (e.g., hyper-high pressures, high temperature) [2] inaccessible for experimental measurement. But they require the potential functions for a wide range of interatomic separations [2]. Thus, interatomic potential plays an important role in solving a wide class of problems in physics, chemistry, and biology.

Theoretically, interatomic potentials can be directly predicted using advanced quantum-chemical approaches, more refined mathematical methods, and high-speed computers [2]. In principle, very accurate potentials can be obtained for a wide range of internuclear distances if sufficient electronic configurations are included in electronic-structure calculations [2]. However, it may be extremely time-consuming and prohibitively expensive in acquiring the interatomic potentials for many-electron systems or weakly bound van der Waals complexes [7]. Nevertheless, advanced experimental techniques, with the help of semi-empirical or empirical analytical potential functions [1], provide another efficient and direct approach to determine very accurate interatomic potentials from the collected spectroscopy, scattering data, or other measurements [1,7].

To date, many interatomic pair-potential functions (see section B.2 List of Pair-Potential Functions in Appendix A) have been reported. All of them can be roughly summarized in five kinds of analytical forms: (i) Dunham-like Taylor expansions, (ii) suitable mathematical functional expressions, (iii) polynomials, (iv) hybrid, and (v) piecewise. The forms (i–iv) with potential parameters calibrated for one property predict other properties inadequately. They focus on describing either strongly or weakly, covalent or ionic bound, neutral, singly-, doubly-, or multiply-charged molecules, and often lose their validity for either small or relatively large internuclear distances. The form (v) uses piecewise analytical forms, in which different potential functions in different ranges of the internuclear distance R are splined together to give a continuous, multi-parameter function defined for all R. Multi-parameter splined functions lack a certain uniqueness [7]. One must make several arbitrary decisions as to where one function ends and the next begins.

On the other hand, an interatomic potential can be expressed in many different analytical functional forms, but all accomplish the same results that are in agreement with experiments [1,2]. In this sense, the agreement between experiment and theory is not a sufficient sign of the correctness and good accuracy of a constructed pair-potential function, but only a necessary condition [1,2], although higher degree of the said agreement may entail much

* Corresponding authors at: Department of Applied Physics, Xi'an Jiaotong University, Xi'an 710049, China. Fax: +1 979 5951189 (R.-H. Xie); fax: +1 435 797 3390 (T. Kar).
E-mail addresses: tapas.kar@usu.edu (T. Kar), rhxie@mail.xjtu.edu.cn (R.-H. Xie).

http://dx.doi.org/10.1016/j.cplett.2014.05.021
0009-2614/

better theory. This is supported by two known facts. The magnitude of the second virial coefficient is not sensitive to the form of the potential-curve shape and its minimum position, but depends only on the ratio between its well width and depth [2]. In the same way, the viscosity coefficient is not sensitive to the dependence of the potential on the separation distance at all [2]. Thus, for practical applications [1–5], is it possible to construct a unique pair-potential function that is able to describe *adequately and accurately* the interatomic potential for a wide range of separations and diatomic systems? In this Letter, we are going to demonstrate the possibility of constructing a generalized interatomic pair-potential function.

2. Generalized pair-potential function

A simple picture of the interatomic potential $V(R)$ for a stable diatomic system [1] presents a function curve with a minimum $V_{\min}$ at the equilibrium internuclear distance R_e, a very sharp rise towards the infinity as $R \to 0$, and a less sharp rise towards the dissociation limit as $R \to \infty$. This establishes the basic criteria [1] that a good interatomic potential must satisfy. In addition, a desirable characteristics of a good potential function is that its analytical formula is flexible enough to describe a unique function that may have more local minima [8] or at least one local maximum and one local/global minimum [6]. Recently, one of us has developed a molecular-orbital-theory based three-parameter pair-potential function (all equations and variables throughout this Letter, except a special note, are in atomic units) [9]

$$E(R) = E_\infty + \frac{J_1(R,\gamma) + K_1(R,\alpha,\beta)}{1 + S_0(R)} \tag{1}$$

with

$$J_1(R,\gamma) = e^{-2\gamma R}\left(\frac{1}{R} + 1\right),$$

$$K_1(R,\alpha,\beta) = e^{-\alpha R}\left(\frac{1}{R} - \beta R\right),$$

$$S_0(R) = e^{-R}\left(1 + R + \frac{R^2}{3}\right),$$

known as the Coulomb, exchange, and overlap integrals, respectively, where α, β, γ are the adjusting parameters, and E_∞ is the total energy of the system at the infinity. We find that this simple function Eq. (1) is able to achieve the criteria and characteristics addressed above. However, Eq. (1) is able to represent only the interatomic potential of the systems with closed-shell and/or *s*-type valence-shell constituents [10], but not for systems having *p*- or *sp*-type valence-shell constituents. Further, the accuracies in the repulsive and attractive regions of this simple model, as pointed out in our recent Letter [11], is not good. If it is able to reach a good accuracy and be applied to a wide range of diatomic systems, this three-parameter potential model will be a good candidate to be used as a base to construct a unique pair-potential function, which is able to describe *adequately and accurately* the interatomic potentials of broad systems for a wide range of R.

The interatomic interactions can be classified according to the three ranges of interatomic separation R [1,2]: (a) a short-R range at which the potential has a repulsive nature and the electronic exchange dominates; (b) an intermediate-R range at which the repulsive and attractive forces reach a balance; and (c) a large-R range at which the electronic exchange is negligible and the intermolecular forces are attractive. In the short-R range, there is no difference between neutral and ion interaction [1]. In the large-R range, however, there are important differences in the functional forms of the interatomic potential [1], for example,

- Neutral closed-shell atoms have a van der Waals (vdW) interaction energy which is asymptotic to the multipolar dispersion expansions, i.e., $-\sum_{n=3}^{\infty}\frac{C_{2n}}{R^{2n}}$ [1,12].
- The interaction of two atomic ions leads to an energy of $\frac{C_1}{R}$ [7].
- An atomic ion interacting with a neutral (non-polar) closed-shell atom will result in an ion-induced dipole interaction energy, $-\frac{Z^2\alpha_1}{2R^4}$ [7]. Higher-order terms include the ion-induced quadrupole and dispersion interaction energy, $-\frac{Z^2\alpha_2}{2R^6} - \frac{C_6}{R^6}$, the ion-induced octopole, ion-hyperpolarizibility, and dispersion interaction energy, $-\frac{Z^2\alpha_3}{2R^8} - \frac{Z^2\gamma_1}{24R^8} - \frac{C_8}{R^8}$, and so on, where Z is the *effective* charge on the atomic ion, α_1, α_2, and α_3 are the dipole, quatrupole, and octopole polarizabilities, respectively, and γ is the second hyperpolarizability.

In the light of these facts, to achieve the adequate range of R, we propose a generalized pair-potential form based on the simple three-parameter potential [9] by adding the asymptotic induction and dispersion terms. Moreover, to accomplish a good accuracy of the three-parameter potential [9] and to extend it to cover a wide range of the diatomic systems (e.g., with p-, sp-type valence-shell constituents), we introduce new parameters η, ζ, and q in the Coulomb $J_1(R)$ and exchange $K_1(R)$ integrals, and consider that parameters α, β, γ, and η all are R-dependent. Thus, we have the generalized interatomic pair-potential function ($V(R) = E(R) - E_\infty$, referencing to E_∞)

$$V(R) = \frac{J_1(R,\gamma',\eta',\zeta,q) + K_1(R,\alpha',\beta',\zeta,q)}{1 + S_0(R)} - I(R,R_e,\chi)\sum_n^{\infty}\frac{C_n}{R^n} \tag{2}$$

with

$$J_1(R,\gamma',\eta',\zeta,q) = e^{-2\gamma' R}\left(\frac{\zeta}{R^q} + \eta'\right),$$

$$K_1(R,\alpha',\beta',\zeta,q) = e^{-\alpha' R}\left(\frac{\zeta}{R^q} - \beta' R\right),$$

$$I(R,R_e,\chi) = N\left(\frac{R}{R_e}\right)\left(1 - e^{-\left(\frac{R}{\chi R_e}\right)^5}\right),$$

where

$$\gamma' = \gamma\left(1 + \sum_{j=1}\lambda_j R^j\right),$$

$$\alpha' = \alpha\left(1 + \sum_{j=1}\kappa_j R^j\right),$$

$$\beta' = \beta\left(1 + \sum_{j=1}\sigma_j R^j\right),$$

$$\eta' = \eta\left(1 + \sum_{j=1}\rho_j R^j\right).$$

The term $N(R/R_e)$ is a sign function defined as $N\left(\frac{R}{R_e}\right) = +1$ (or -1) if $R/R_e \geqslant 10^{-3}$ (or $R/R_e < 10^{-3}$), where R_e is the equilibrium distance. The number n in Eq. (2) is defined specifically by studied cases, for example, $n = 6, 8, \ldots$for neutral closed-shell atoms. The asymptotic $-\frac{C_n}{R^n}$ term has an improper behavior in that it goes to $-\infty$ as $R \to 0$. This is due to the asymptotic nature of the induction and/or dispersion expansions, which are only valid for the internuclear distances in which charge distributions do not overlap. To eliminate the unrealistic behavior, a damping term similar to Ref. [13], $1 - e^{-\left(\frac{R}{\chi R_e}\right)^5}$ with a damping parameter χ and a sign function $N\left(\frac{R}{R_e}\right)$, is introduced in front of the sum of $\frac{C_n}{R^n}$ terms.

To process the experimental or *ab initio* data, the analytical form of this interatomic pair-potential function Eq. (2) depends upon

the case under study. In the following, we discuss specifically five cases.

2.1. Covalent bonding: neutral systems

Covalent bonding is the sharing of electrons between atoms. Its binding energy is typically on the order of electron volts (eV) (hydrogen bonds are about an order of magnitude weaker, and vdW bonds are much weaker). First, we apply the new potential function Eq. (2) to represent neutral covalent bonding systems. For practical applications [2], we keep in mind throughout this Letter that the potential function must involve as few as possible potential parameters. For neutral covalent bonding systems, we set, in general, $\gamma = 2\alpha,\ \zeta = q = 1,\ \lambda_1 = \kappa_1 = \kappa,\ \lambda_j = \kappa_j = 0$ ($j \geqslant 2$ integer), and $\rho_j = \sigma_j = 0$ ($j \geqslant 1$ integer), and do not include the induction and dispersion terms. Then, we have a four-parameter ($\alpha,\ \beta,\ \eta,\ \kappa$) interatomic pair-potential function for neutral covalent systems

$$V(R) = \frac{J_1(R,\alpha,\kappa,\eta) + K_1(R,\alpha,\kappa,\beta)}{1 + S_0(R)} \tag{3}$$

with

$$J_1(R,\alpha,\kappa,\eta) = e^{-4\alpha R(1+\kappa R)}\left(\frac{1}{R} + \eta\right),$$

$$K_1(R,\alpha,\kappa,\beta) = e^{-\alpha R(1+\kappa R)}\left(\frac{1}{R} - \beta R\right).$$

2.2. Covalent bonding: ionic systems

For ionic covalent-bonding systems, we define $q = 1$, and $\lambda_j = \kappa_j = \rho_j = \sigma_j = 0$ ($j \geqslant 1$ integer). In the long range, as addressed before, it may include the terms [7] of $\frac{C_1}{R}$, $-\frac{Z^2\alpha_1}{2R^4}, -\frac{Z^2\alpha_2}{2R^6} - \frac{C_6}{R^6} - \frac{Z^3\alpha_2'}{2R^7}, -\frac{Z^2\alpha_3}{2R^8} - \frac{Z^4\gamma_1}{24R^8} - \frac{C_8}{R^8}$ (α_2' is the dipole-quadrupole polarizability). For convenience, we designate them as $\frac{C_1}{R}$, $\frac{C_4}{R^4}, \frac{C_6}{R^6}, \frac{C_7}{R^7}, \frac{C_8}{R^8}$ with only a single parameter C_n for each $\frac{C_n}{R^n}$ term. Thus, the potential function is

$$V(R) = \frac{J_1(R,\gamma,\zeta,\eta) + K_1(R,\alpha,\zeta,\beta)}{1 + S_0(R)} - I(R,R_e,\chi)\sum_n \frac{C_n}{R^n} \tag{4}$$

with

$$J_1(R,\gamma,\zeta,\eta) = e^{-2\gamma R}\left(\frac{\zeta}{R} + \eta\right),$$

$$K_1(R,\alpha,\zeta,\beta) = e^{-\alpha R}\left(\frac{\zeta}{R} - \beta R\right).$$

2.3. Ionic bonding systems

Ionic bonding, a type of chemical bond that generates two oppositely charged ions, is a complete transfer of valence electron (s) between atoms. Thus, the net charge of the compound (e.g., NaCl, KCl) must be zero. Pure ionic bonding cannot exist. The term *ionic bonding* is given when the ionic character is greater than the covalent character. Thus, it is necessary to involve the covalent character in developing a model potential for ionic bonding systems. The pair potential functions such as Rittner, Varshni-Shukla, and Bellert-Breckenridge potentials listed in Appendix A were developed only for pure ionic bonding systems by combining a Born–Mayer [14] repulsive term with the induction and dispersion terms. Here we apply the generalized potential function Eq. (2) to describe the ionic bonding systems. The proposed potential function is the same as Eq. (4).

2.4. Weakly bound van der Waals systems

One can discuss diatomic bonds by means of the virial theorem [7]. Weakly bound vdW diatomic systems establish their equilibrium positions over a relatively shorter distance (measured in the units of R_e) than do chemically bond molecules, and the onset of repulsion is relatively more abrupt for a weak bond. These effects are what one expects in the absence of extensive charge delocalization during bonding [7]. However, the partially covalent nature has been shown in vdW diatomic systems such as NaAr, LiHg, and XeF [7]. As demonstrated in Ref. [10], the potentials of the ground states of the strongly and weakly bound molecules in the potential-well region can be described approximately by a single reduced binding-energy relation [10], i.e., a reduced Rydberg function, $-(1+\sqrt{2}R^*)e^{-\sqrt{2}R^*}$, where $R^* = \frac{R-R_e}{L_2}$ and $L_2 = \sqrt{\frac{2D_e}{f_2}}$ (D_e, the dissociation energy; f_2, the second force constant). This reduced function is also a good representation of the potential curves of covalently bonded materials [10]. In this sense, the partially covalent nature should be considered in developing a pair-potential function for weakly bounded vdW complexes. Thus, for the vdW systems, we define $\gamma = \alpha, \zeta = q = 1$, and $\lambda_j = \kappa_j = \rho_j = \sigma_j = 0$ ($j \geqslant 1$ integer). The potential function in terms of the long-range expansions of electrostatic, induction and dispersion interactions is

$$V(R) = \frac{J_1(R,\alpha,\eta) + K_1(R,\alpha,\beta)}{1 + S_0(R)} - I(R,R_e,\chi)\sum_n^{\infty} \frac{C_n}{R^n} \tag{5}$$

with

$$J_1(R,\alpha,\eta) = e^{-\alpha R}\left(\frac{1}{R} + \eta\right),$$

$$K_1(R,\alpha,\beta) = e^{-\alpha R}\left(\frac{1}{R} - \beta R\right).$$

Different from our recent Letter [15] where $J_1(R,\gamma,\eta) = e^{-2\gamma R}(\frac{1}{R} + \eta)$, the above potential function Eq. (5) has reduced the parameter γ to α, i.e., setting $\gamma = \alpha/2$. To be noted, if the coefficients C_n are not available in the literature, they can be used as adjusting parameters (see the case study of $LiHe^-$ in Section 4.6.3 in Appendix A). In fact, Eq. (5) can be re-organized as follows

$$V(R) = P(R)\frac{e^{-\alpha R}}{R} + Q(\eta,R)e^{-\alpha R}(1 - \beta^* R) - I(R,R_e,\chi)\sum_n^{\infty}\frac{C_n}{R^n} \tag{6}$$

with $P(R) = \frac{2}{1+S_0(R)}$, $Q(\eta,R) = \frac{\eta}{1+S_0(R)}$, and $\beta^* = \frac{\beta}{\eta}$. The first term, $P(R)\frac{e^{-\alpha R}}{R}$ in Eq. (6), is a Pauli-type potential, but with an R-dependent coefficient $P(R)$. Hellmann (1935), Frost-Musulin (1954), Frost-Woodson (1958), Varshni-Shukla III (1965) potentials and Buckingham (1958) repulsive potential (see the potential list in Appendix A) have the Pauli-type repulsion term. The second term, $Q(\eta,R)e^{-\alpha R}(1-\beta^* R)$, is the Rydberg (1931) potential listed in Appendix A, but with an R- and η-dependent coefficient $Q(\eta,R)$. Thus, we also call this newly constructed potential function Eq. (5) or Eq. (6), Pauli-Rydberg-vdW (PRvdW) potential. Further, the above Eq. (6) includes a Born–Mayer repulsive term, $Q(\eta,R)e^{-\alpha R}$ [14], but with an R- and η-dependent coefficient $Q(\eta,R)$. To be noted, the well-known Tang-Toennies potential [12], $V(R,A,b) = Ae^{-bR} - \sum_{n\geqslant 3} f_n(b,R)\frac{C_{2n}}{R^{2n}}$ where $f_n(b,R)$ is a damping function, employs the Born–Mayer potential Ae^{-bR} as the repulsive term, but with a constant coefficient A.

2.5. Meta-stable systems

The diatomic dications, XY^{++}, are widely described by two possible situations, corresponding to the attractive ($X^{++} + Y$) and repulsive ($X^+ + Y^+$) dissociation limits [6]. The polarization of Y by X^{++} always leads to attractive interactions. Coulomb repulsion is

always present, and in addition, covalent bonding for some molecules may exist between two mono-positive atomic ions. In general, such bonding interactions may lead to meta-stable potentials which have a local minima and a barrier. Here we demonstrate that the new potential form Eq. (2) with only five parameters α, β, γ, ζ and q (setting $\eta = 1, \lambda_j = \kappa_j = \rho_j = \sigma_j = 0$, $j \geqslant 1$ integer,) and without including the induction and dispersion terms is able to represent accurately the potential curves of meta-stable diatomic systems. The proposed potential function for meta-stable diatomic dications is

$$V(R) = \frac{J_1(R,\gamma,\zeta,q) + K_1(R,\alpha,\beta,\zeta,q)}{1 + S_0(R)}, \tag{7}$$

with

$$J_1(R,\gamma,\zeta,q) = e^{-2\gamma R}\left(\frac{\zeta}{R^q} + 1\right),$$

$$K_1(R,\alpha,\beta,\zeta,q) = e^{-\alpha R}\left(\frac{\zeta}{R^q} - \beta R\right).$$

3. Results and discussions

In Appendix A, we provide details on the case study and Fortran 90 source codes for determining the potential parameters. All parameters for the case study are summarized in Appendix A (Table A1, A2, A3, A4). To be noted, for cases that are not fitted in any of the five cases, the generalized function form Eq. (2) can be applied directly.

3.1. Covalent bonding: neutral systems

In Section 1 of Appendix A, we have demonstrated that Eq. (3) is able to describe accurately the potentials of the ground states of diatomic molecules (e.g., H_2, B_2, Li_2, C_2, N_2, F_2, Si_2, HCl, LiH, BeH, CH, NH, OH, InH, CO, NO, SiO, LiNa) with *p*- and *sp*-type valence-shell constituents as well as closed-shell and *s*-type valence-shell constituents for a wide range of *R*. All parameters for this case study are summarized in Table A1 of Appendix A.

Here we take the ground state of H_2 as an example. We first compute the potential energy of the ground-state H_2 by using the couple cluster method with single and double excitation (CCSD) [16] and basis set aug-cc-pV5Z (augmented correlation-consistent core-valence basis sets up to quintuple-zeta quality) implemented in GAUSSIAN 09 package [17]. As shown in Figure 1, our CCSD/aug-cc-pV5Z calculations are in excellent agreement with the exact data [18]. Then, we fit the CCSD/aug-cc-pV5Z data by using Eq. (3). The Root-Mean-Square (RMS) for this fitting is 0.00046, and four potential parameters are determined to be $\alpha = 1.24179616$, $\beta = 1.91867424$, $\kappa = 0.0478910411$, and $\eta = 2.8004031$. Figure 1 presents our fitted potential energy curve (PEC), which agrees well

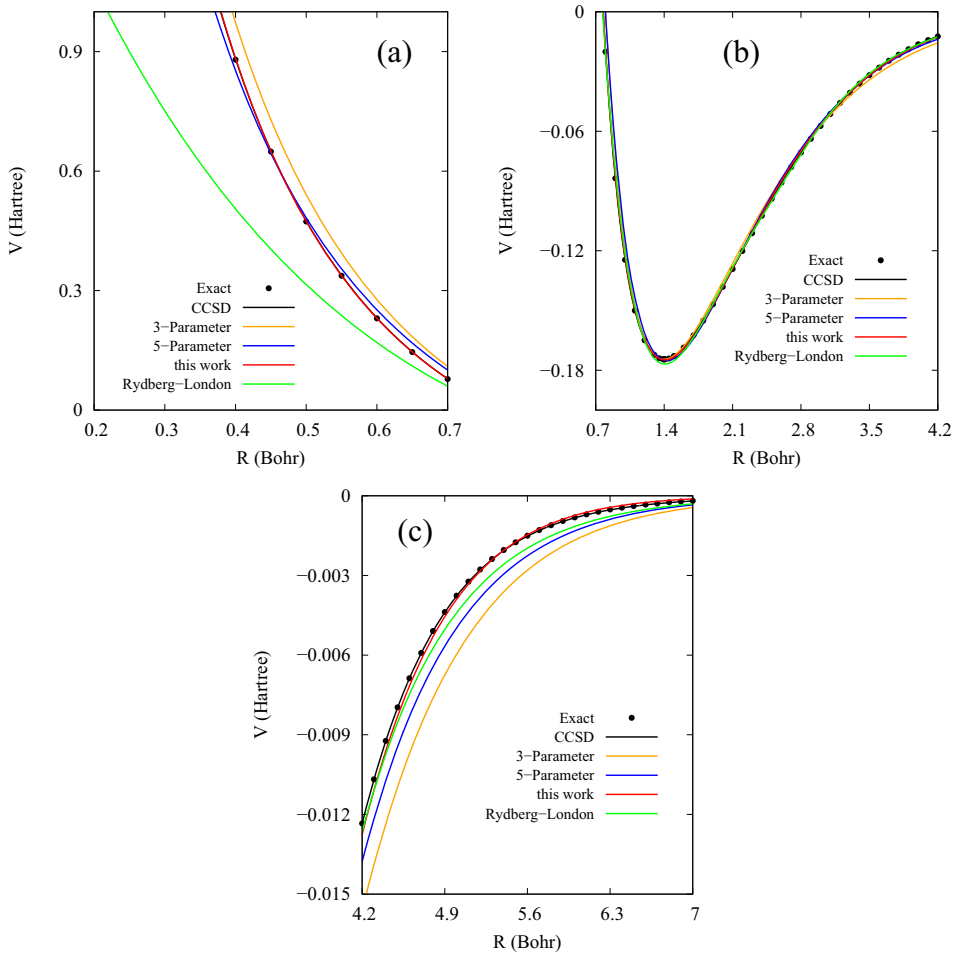

Figure 1. The comparison between 4-parameter potential (this Letter) (Red line, $\alpha = 1.24179616$, $\beta = 1.91867424$, $\kappa = 0.0478910411$, and $\eta = 2.8004031$), 3-parameter potential (Orange line, Ref. [9], $\alpha = 1.5065756$, $\beta = 2.48475652$, and $\gamma = 1.45$), 5-parameter potential (Blue line, Ref. [11], $\alpha = 1.519$, $\beta = 2.0478$, $\gamma = 1.785$, $n = 0.795$, $\zeta = 1.005$), Rydberg-London potential (Green line, Ref. [19], $a = 53.8$, $b = 2.99$, $c = 2.453$, $d = 3.884$, and $e = 47.6$), CCSD/aug-cc-pV5Z (Dark line), and the exact data (Dark filled circles, Ref. [18]) for the ground state of H_2: (a) Short-R; (b) Intermediate-R; (c) Large-R regions. To be noted, CCSD results in (a) overlap with the four-parameter potential. (For interpretation of the references to colour in this figure legend, the reader is referred to the web version of this article.)

with the exact data [18]. Also, in the short- and large-R regions, as shown in Figure 1a and c, respectively, our four-parameter potential is greatly improved in accuracy over the three-parameter [9] and and five-parameter [11] potentials.

Ten years ago, Cahill and Parsegian [19] demonstrated that their constructed five-parameter Rydberg-London (RL) potential for the ground-state H_2 is five times more accurate than Morse [20], Varshni [21], and Hulburt–Hirschfelder [22] potentials, and are four orders of magnitude more accurate than Lennard-Jones (LJ) [23] and harmonic potentials. In Figure 1, we compare our four-parameter potential with RL potential. In the intermediate-R region (Figure 1b), RL potential except a visible deviation in the bottom of the potential well overlaps with our four-parameter potential curve. However, RL potential [19] is much softer in the short-R region (Figure 1a) than our four-parameter potential, and displays a discernible deviation in the large-R region (Figure 1c). It concludes that our four-parameter potential is more accurate than five-parameter RL potential.

Rydberg–Klein–Rees (RKR) [24–26] turning points and vibrational levels provide accurate reference standards for assessing the quality of a potential-energy curve [1]. Thus, we have calculated the vibrational energies for the ground-state H_2 by using the four-parameter potential function. The numerical results are summarized in Table 1 and compared with the literature data. We find that our computed vibrational energies are within a relative error of less than 1% and 3% for the vibrational levels $v = 0, 1, \ldots, 12$ and $v = 13, 14$ levels, respectively, compared to experiment [27]. It shows that the present four-parameter potential is more accurate than three-parameter [9], five-parameter [11], and RL [19] potentials.

3.2. Covalent bonding: ionic systems

The long-range ion/induced-dipole force (represented by $\frac{C_4}{R^4}$ term) is a major attractive force between atomic ion and neutral atom, especially at a large R. In Section 2 of Appendix A, we have demonstrated that Eq. (4), with the inclusion of $-\frac{C_4}{R^4}$ only, is able to describe accurately and adequately the potentials of the ground states of covalently bounded HeH^+, H_2^+, He_2^+, BeH^+, BeH^-, and LiH^- for a wide range of R. All parameters for this case study are summarized in Table A2 of Appendix A. Here we present the results of HeH^+.

According to the standard Big Bang model, the helium hydride ion, HeH^+, is the first molecule, formed in the Universe. This HeH^+ is a relatively simple hetero-nuclear molecular ion, isoelectronic with H_2, which makes it of a fundamental significance from the theoretical point of view. The first accurate variational calculations of the Born–Oppenheimer potential of HeH^+ was reported by Wolniewicz [28], and then refined by Kolos and Peek [29]. To date, there have been extensive quantum chemical calculations on this system (see literature review in Ref. [30,31]). In the ground electronic state, both electrons are mostly centered around the α nucleus with the proton distance from α being about $R \approx 1.46$ Bohr. Very recently, Pachucki [31] has demonstrated high accuracy calculations for the the ground state of HeH^+ using analytic formulas for two-center two-electron integrals with exponential functions (The potential is obtained in the range of 0.1∼60 a.u. with precision of about 10^{-12} a.u.).

In this Letter, we first compute the PEC of the ground state of HeH^+ using CCSD/aug-cc-pV5Z and then fit it using the new potential function given by Eq. (4). The RMS for this fitting is 0.0003, and the potential parameters are determined to be $\alpha = \gamma = 1.94869912$, $\beta = 2.60094136$, $\zeta = 2.04347269$, $\eta = 1.78190656$, $C_4 = 0.709265297$, and $\chi = 2.64764358$. Since $C_4 = \alpha_1/2$, the dipole polarizability of He atom is derived to be $\alpha_1 = 2C_4 = 1.418530594$, which agrees well with the literature value ($\alpha_1 = 1.3796$, or 1.4870) [32]. The fitting results are presented in Figure 2. The fitted PEC except a slight deviation at $R = 4 \sim 6$ Bohr shown in Figure 2c overlap very well with CCSD/aug-cc-pV5Z data points and the most accurate data [31]. The new potential curve is greatly improved in accuracy over the three-parameter potential curve [9] in the repulsive and attractive regions.

We calculate the vibrational energies for the ground state HeH^+, and the numerical results are summarized in Table 2. In total, we have obtained 12 vibrational levels as reported in Ref. [30,31,33]. The relative error of calculated vibrational energies by using the present potential are less than 2% for all the levels $v = 0 - 11$, compared to the accurate data [31].

3.3. Ionic bonding systems

Taking the ground state of NaCl as an example, we fit its experimentally determined potential [34]. The RMS for this fitting is 0.00248 (here C_4, C_6, and C_7 are taken as fitting parameters). The fitted potential curve, as shown in Figure 3, agrees well with experiment [34]. The computed vibrational energies for isotopes $Na^{35}Cl$

Table 1
The calculated vibrational energies for the ground state of H_2 using four-parameter (this Letter, $\alpha = 1.24179616$, $\beta = 1.91867424$, $\kappa_1 = 0.0478910411$, and $\eta = 2.8004031$), three-parameter [9] ($\alpha = 1.5065756$, $\beta = 2.48475652$, $\gamma = 1.45$), five-parameter [11] ($\alpha = 1.519$, $\beta = 2.0478$, $\gamma = 1.785$, $n = 0.795$, $\zeta = 1.005$), and Rydberg-London [19] ($a = 53.8$, $b = 2.99$, $c = 2.453$, $d = 3.884$, and $e = 47.6$) potentials. The value in the parenthesis is the relative error ($\delta = \frac{|Theory - Experiment|}{Experiment}$) of the calculation, compared to experiment [27].

v	Exp. (Ref. [27]) [eV]	Three-parameter (Ref. [9]) [eV] (%)	Five-parameter (Ref. [11]) [eV] (%)	Rydberg-London (Ref. [19]) [eV] (%)	Four-parameter (**this Letter**) [eV] (%)
0	−4.4774	−4.4628 (0.33)	−4.4849 (0.17)	−4.5247 (1.06)	−4.4852 (0.17)
1	−3.9615	−3.9218 (1.00)	−3.9500 (0.29)	−3.9779 (0.41)	−3.9661 (0.12)
2	−3.4747	−3.4166 (1.67)	−3.4457 (0.83)	−3.4729 (0.05)	−3.4750 (0.01)
3	−3.0166	−2.9465 (2.32)	−2.9724 (1.46)	−3.0101 (0.22)	−3.0123 (0.14)
4	−2.5866	−2.5111 (2.92)	−2.5307 (2.16)	−2.5856 (0.04)	−2.5783 (0.32)
5	−2.1847	−2.1099 (3.42)	−2.1211 (2.91)	−2.1899 (0.24)	−2.1734 (0.52)
6	−1.8110	−1.7427 (3.77)	−1.7442 (3.69)	−1.8169 (0.33)	−1.7981 (0.71)
7	−1.4661	−1.4093 (3.87)	−1.4008 (4.46)	−1.4673 (0.08)	−1.4532 (0.88)
8	−1.1508	−1.1097 (3.57)	−1.0916 (5.14)	−1.1460 (0.43)	−1.1396 (0.97)
9	−0.8665	−0.8439 (2.61)	−0.8178 (5.62)	−0.8578 (1.00)	−0.8583 (0.94)
10	−0.6153	−0.6123 (0.49)	−0.5804 (5.68)	−0.6068 (1.38)	−0.6109 (0.71)
11	−0.4000	−0.4155 (3.88)	−0.3806 (4.84)	−0.3957 (1.08)	−0.3994 (0.14)
12	−0.2245	−0.2543 (13.27)	−0.2203 (1.89)	−0.2271 (1.16)	−0.2266 (0.93)
13	−0.0945	−0.1301 (37.67)	−0.1013 (7.16)	−0.1031 (9.10)	−0.0966 (2.25)
14	−0.0174	−0.0452 (159.77)	−0.0264 (51.78)	−0.0264 (51.72)	−0.0169 (2.73)

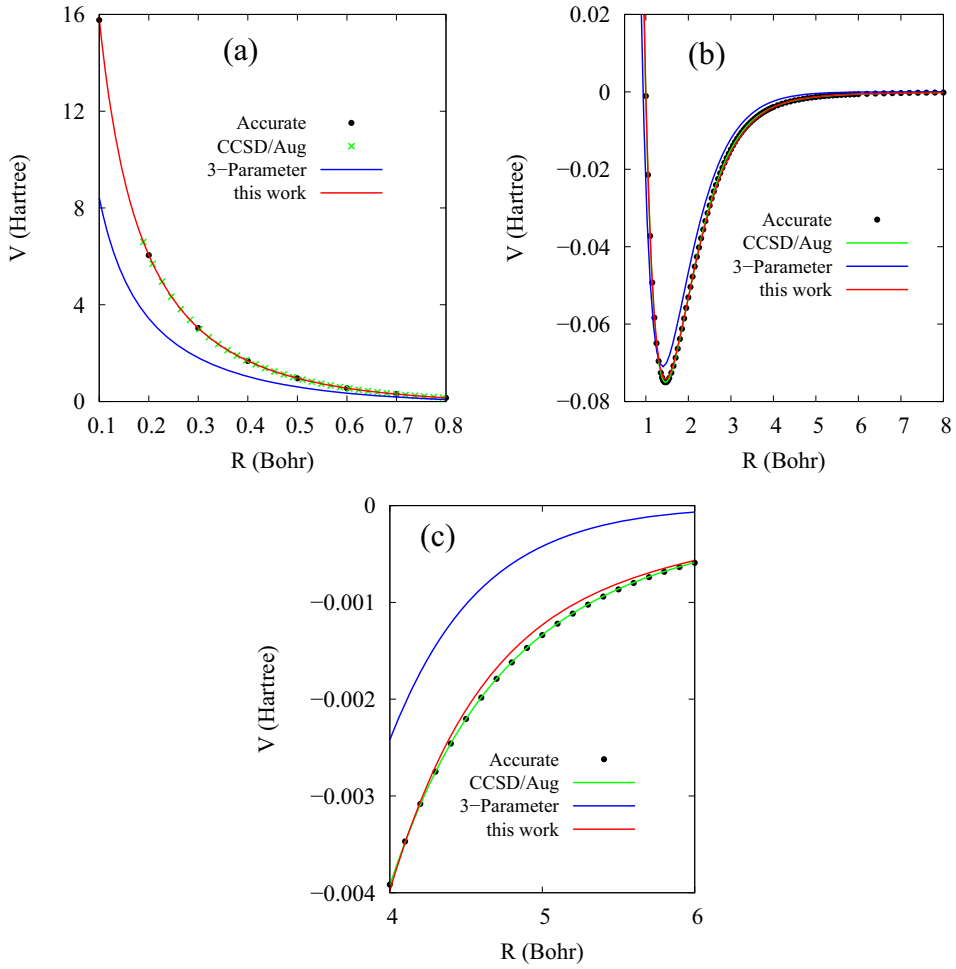

Figure 2. The comparison between the present potential (this Letter) (Red line, $\alpha = \gamma = 1.94869912$, $\beta = 2.60094136$, $\zeta = 2.04347269$, $\eta = 1.78190656$, $C_4 = 0.709265297$, $\chi = 2.64764358$, and $R_e = 2.042$), CCSD/aug-cc-pV5Z (Green line or crossing), 3-parameter potential (Blue line, $\alpha = 2.087114$, $\beta = 3.54492339$, and $\gamma = 1.0$, Ref. [9]), and the most accurate data (Dark filled circles, Ref. [31]) for the ground state of HeH^+: (a) Repulsive region; (b) Attractive region, and (c) an enlarged part in (b). (For interpretation of the references to colour in this figure legend, the reader is referred to the web version of this article.)

Table 2
Comparison of the vibrational energies for the ground state of HeH^+ calculated using the present potential (this Letter) ($\alpha = \gamma = 1.94869912$, $\beta = 2.60094136$, $\chi = 2.04347269$, $\eta = 1.78190656$, $C_4 = 0.709265297$, $\zeta = 2.64764358$, and $R_e = 2.042$). The value in the parenthesis is the relative error ($\delta = \frac{|\text{Theory}-\text{Accurate}|}{\text{Accurate}}$) of the calculation, compared to the most accurate data [33]. Energies in cm^{-1}

v	This Letter	Accurate (Ref. [33])	v	This Letter	Accurate (Ref. [33])
0	0.	0.	6	12553.3559 (1.78%)	12781.3485
1	2868.9228 (1.45%)	2911.0174	7	13563.0243 (1.47%)	13765.8454
2	5422.8349 (1.68%)	5515.2227	8	14250.4013 (1.07%)	14405.1903
3	7666.1656 (1.85%)	7810.8577	9	14607.3517 (0.85%)	14732.6855
4	9601.9423 (1.95%)	9792.9915	10	14722.6704 (0.85%)	14848.9097
5	11231.4052 (1.94%)	11453.4425	11	14748.7441 (0.84%)	14873.3489

and $Na^{37}Cl$ listed in Table 3.1 of Appendix A are also in good agreement with experimentally determined energies [34].

3.4. Weakly bound van der Waals systems

In Section 4 of Appendix A, we have successfully applied Eq. (5) to describe accurately the triplet states of the weakly bounded H_2 and NaK, and the ground states of 25 weakly bounded vdW complexes such as rare-gas dimers (He_2, Ne_2, Ar_2, Kr_2, Xe_2), alkaline-earth dimers (Mg_2, Ca_2, Sr_2), metal-rare gas dimers (LiHe, LiAr, NaAr, KAr, NaKr, CaHe), group 12 dimers (Zn_2, Cd_2, Hg_2), rare-gas halides (XeF, KrF), and others (LiHg, CdNe, HeH, NeH, AgHe, $LiHe^-$) for a wide range of R. All parameters for this case study are summarized in Table A3 of Appendix A. Here we present Ar_2 and Mg_2 as two examples.

The interatomic potential for the ground state of Ar_2 is as well characterized as that for many common stable diatomics, experimentally by using several spectroscopic techniques and theoretically by using *ab initio* techniques [35]. The most accurate potential energy curve of its ground state was experimentally determined by Aziz [36]. Thus, we use Eq. (5) and the dispersion coefficients C_6, C_8 and C_{10} of Ref. [37] to fit directly the accurate data of Aziz [36]. The RMS of this fitting is 0.0151, and the potential parameters are determined to be $\alpha = 1.5069144$, $\beta = 19.2457331$, $\eta = 126.019972$, and $\chi = 1.28100922$. Our fitted potential curve is

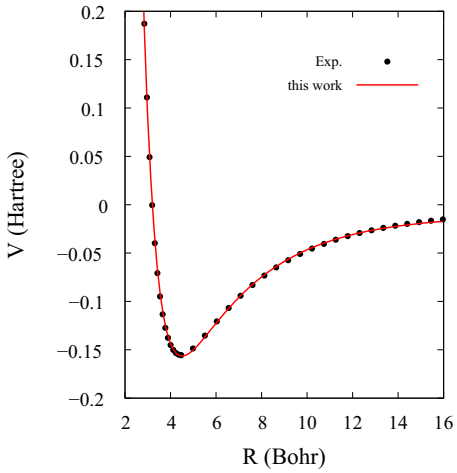

Figure 3. The comparison between the present potential (this Letter) (Red line, $\alpha = \gamma/2 = 0.449611907$, $\beta = 0.130590627$, $\eta = 125.509261$, $\chi = 7.29009261$, $R_e = 4.4628$, $C_4 = 2.09988569 \times 10^{-6}$, $C_6 = 2008637.94$, $C_7 = 99999986.1$, and $\zeta = 1$) and the experimental data (Dark filled circles, Ref. [34]) for the ground state of NaCl. (For interpretation of the references to colour in this figure legend, the reader is referred to the web version of this article.)

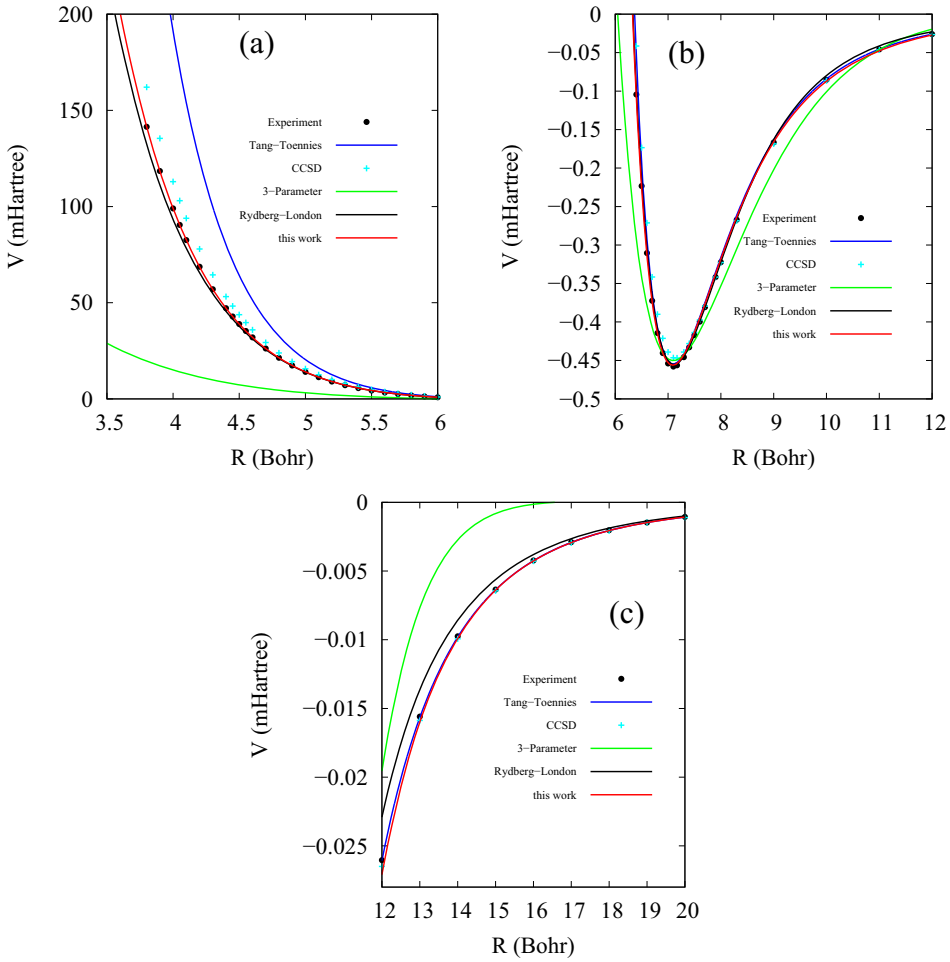

Figure 4. Comparison of the ground-state potential curve of Ar_2: The present Letter (this Letter) (Red line, $\alpha = 1.5069144$, $\beta = 19.2457331$, $\eta = 126.019972$, $\chi = 1.28100922$, $R_e = 7.10$, $C_6 = 64.3$, $C_8 = 1623$, and $C_{10} = 49060$) with CCSD/daug-cc-pV5Z-33211 calculations (Cyan cross, Ref. [35]), experimental data (Dark filled circles, Ref. [36]), Tang-Toennies potential (Blue line, $A = 748.3$, $b = 2.031$, $C_6 = 64.3$, $C_8 = 1623$, and $C_{10} = 49060$, Ref.[37]), Rydberg-London potential (Dark line, $a = 1720$, $b = 2.6920$, $c = 0.2631$, $d = 37.943$, $e = 177588$, Ref. [19]), and three-parameter potential (Green line, $\alpha = 0.8706$, $\beta = 0.403498$, $\gamma = 0.38$, Ref. [9]). (a) Short-R; (b) Intermediate-R; (c) Large-R. (For interpretation of the references to colour in this figure legend, the reader is referred to the web version of this article.)

presented in Figure 4, which agrees very well with the accurate data [36]. As shown in Figure 4a), Tang-Toennies potential [37] is much harder, and CCSD/daug-cc-pV5Z-33211 calculations [35] is slightly harder than the accurate data [36]. Overall, the new potential is greatly improved in accuracy over the three-parameter potential [9] in all the regions.

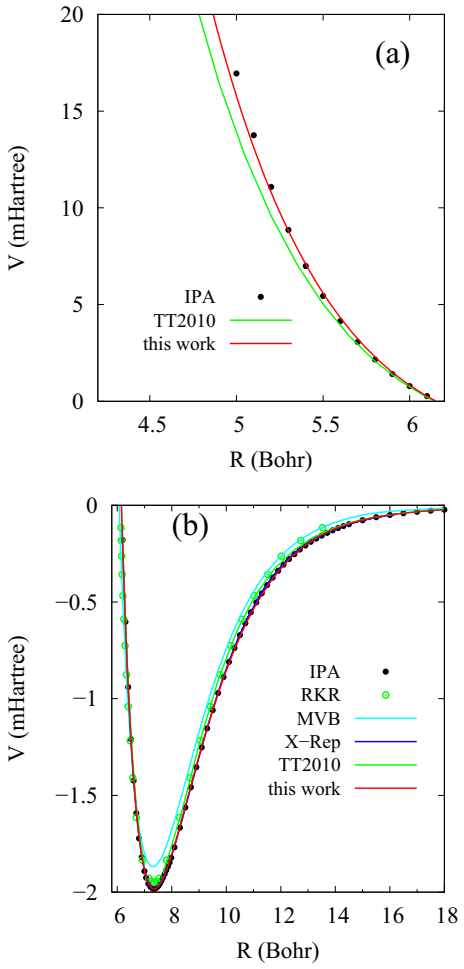

Figure 5. Comparison of the ground-state potential curve of Mg_2: The present Letter (this Letter) (Red line, $\alpha = 1.24946345$, $\beta = 2.67596495$, $\eta = 29.910735$, $\chi = 1.34122874$, $R_e = 7.354$, $C_6 = 627$, $C_8 = 41500$, and $C_{10} = 2757000$) with the RKR data points (Green open circles, Ref. [39]), IPA potential (Dark filled circles, Ref. [40]), X-representation of the potential energy curves (Blue line, Ref. [41]), Tang-Toennies potential (Green line, $A = 7.3486$, $b = 1.0475$, $C_6 = 627$, $C_8 = 41500$, and $C_{10} = 2757000$, Ref.[42]), and *ab initio* multi-configuration valence bond (MVB) calculation (Cyan line, Ref. [43]). (a) Repulsive and (b) Attractive regions. (For interpretation of the references to colour in this figure legend, the reader is referred to the web version of this article.)

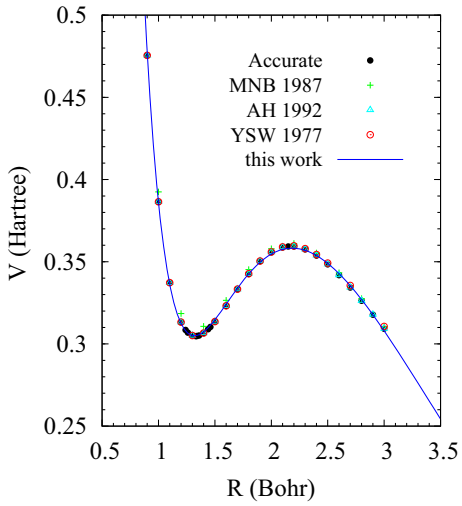

Figure 6. The comparison between the present five-parameter potential (this Letter) (Blue line, $\alpha = 2.19893097$, $\beta = 21.3316218$, $\gamma = 0.279984035$, $\zeta = 3.6828207$, and $q = 0.712005705$), full CI calculation (AH 1992) (Cyan triangle, Ref. [47]), multi-reference double excitation CI calculation (MNB 1987) (Green cross, Ref. [46]), a James-Coolidge-method based calculation (YSW 1977) (Red open circles, Ref. [45]), and the most accurate data (Dark filled circles, Ref. [48]) for the meta-stable diatomic dication, He_2^{++}. The potential-well minimum located at $R_{min} = 1.333$ Bohr, and the barrier at $R_{max} = 2.184$ Bohr with a height of 0.05677 Hartree. (For interpretation of the references to colour in this figure legend, the reader is referred to the web version of this article.)

Cahill and Parsegian [19] have compared Rydberg-London (RL) potential for the ground-state Ar_2 with Lennard-Jones (LJ) potential [23]. They pointed out that the LJ potential curve matched at the potential minimum is too deep for $R > 8.5$ Bohr, and too hard for $R < 5.671$ Bohr [19]. Does it matter that LJ fails to fit the Ar-Ar interaction? Cahill and Parsegian [19] found that the dimensionless second virial coefficient B_2/R_e^3 of Ar_2 calculated by using RL and LJ potentials at room temperature are -0.499 and -0.899, which differ from the experimental value of -0.552 [38] by 9.6% and 63%, respectively. Thus, LJ fitting with only two parameters is not as accurate as RL fitting [19].

Then, is the accuracy of RL potential important in the liquid phase where additivity is only approximate? Cahill and Parsegian [19] have significantly tested whether the lack of complete additivity in the liquid phase obscures the advantages of the RL potential over the LJ potential. They calculated the heats of vaporization $\Delta_{vap}H$ of Ar at the boiling points and atmospheric pressure by using RL and LJ potentials in Monte Carlo simulation [19]. RL and LJ potentials gave $\Delta_{vap}H = 0.0694, 0.0787$ eV (per atom), which differ from the experimental value of 0.0666 eV [38] by 4.2% and 18%, respectively. Clearly, the errors due to a lack of additivity are of the order of 4% [19], while the errors due to the defect of the LJ potential are about 18% [19]. Their analysis has shown that even in the liquid phase, limited additivity is less of a problem than the defects of the LJ potential [19]. Thus, they concluded that RL potential represents weak noncovalent bonds better than LJ potential [19].

How is the accuracy of our new potential function Eq. (5), compared to RL potential? In the intermediate-R region, as shown in Figure 4b, RL potential curve except a visible deviation at $10 < R < 12$ overlaps well with our potential curve and the accurate data. In the repulsive region shown in Figure 4a, RL curve is slightly softer than the accurate data and our potential (to be noted, RL converges to a finite value as R goes to 0). In the large-R region shown in Figure 4c, RL potential displays a discernible deviation at $R = 12 \sim 16$ Bohr. It shows that our potential function is more accurate than RL potential (same conclusion drawn for Kr_2 reported in Section 4.2.4 of Appendix A). Thus, the relative error 4.2% [19] of the calculated heats of vaporization $\Delta_{vap}H$ of Ar at the boiling points and atmospheric pressure by using the Rydberg-London potential [19], due to the lack of additivity, can be further reduced by using our new potential function Eq. (5).

Further, we calculate the vibrational energies for the ground state of Ar_2 using the new potential function. The results are summarized in Table 4.2.3 of Appendix A and compared with those obtained by using other potential functions. Our results are in excellent agreement with experiment [36], and are more accurate than those obtained by using RL [19], Tang-Toennies [12], and Lennard-Jones [23] potentials.

For Mg_2, there are several ways to obtain the interaction potential of its ground-state. First, a Rydberg–Klein–Rees (RKR) potential [39] has been constructed from the measurement of the rovibrational levels. Second, Vidal and Scheingraber [40] have improved upon the RKR analysis [39] by applying a variational procedure based on the inverted perturbation approach (IPA). As shown in

Figure 5, there is a slight difference between RKR and IPA data points in the attractive region. Very recently, Tiemann group [41] has investigated the $A^1\sum_u^+$-$X^1\sum_g^+$ UV spectrum of Mg_2 with high resolution Fourier-transform spectroscopy, and achieved a very accurate PEC for the ground-state Mg_2, i.e., the X-representation PEC shown in Figure 5, which overlaps exactly with the IPA data points. Using Eq. (5) and the dispersion coefficients C_6, C_8 and C_{10} of Ref. [41], we fit the accurate potential data of Ref. [41]. The RMS of this fitting is 0.00534, and the potential parameters are determined to be $\alpha = 1.24946345$, $\beta = 2.67596495$, $\eta = 29.910735$, and $\chi = 1.34122874$. Figure 5 presents our fitted PEC. Except a slight deviation in the repulsive region, the fitted PEC overlaps well with the IPA points. To be noted, Tang-Toennies potential [42] is getting softer and softer in the repulsive region (see Figure 5a) as R decreases, and shows a slight deviation from the IPA points in the attractive region. In comparison with the other PECs, *ab initio* multi-configuration valence bond (MVB) calculation [43] shows some deviations from the IPA data points[40] and X-representation PEC [41], but is close to the RKR points [39].

Finally, it should be mentioned that the potential function Eq. (5) (or Eq. (6)) is also able to represent accurately the ground-state potentials of charged vdW diatomic systems. As an example, we present a case study of $He+Li^-$ in Section 4.6.3 of Appendix A.

3.5. Meta-stable systems

The dication molecule, He_2^{++}, was the first doubly positively-charged diatomics predicted to be meta-stable by Pauling [44], and has been serving as a prototype for studies of bonding in dications [45–49]. Thus, we take it as an example (see Section 5.2 and 5.3 in Appendix A for two hetero-nuclear dications, BeH^{++} and AlH^{++}, respectively. All parameters for this case study are summarized in Table A4 of Appendix A). We fit the most accurate data of Wolniewicz [48], and the RMS for this fitting is 0.00581. Figure 6 reports the fitted potential curve and is compared with the accurate data [48] and several full configuration interaction (CI) [46], multi-reference double excitation CI [47], and a James-Coolidge-method based [45] calculations. We found that Eq. (7) fits very well the accurate data and other calculations. Thus, the constructed pair-potential function Eq. (7) represents accurately the meta-stable state of He_2^{++}: a potential well with a minimum energy of 0.303744 Hartree located at $R_{min} = 1.333$ Bohr, and a potential barrier of 0.05677 Hartree located at $R_{max} = 2.184$ Bohr. The spacings of our computed vibrational energies for $^4He_2^{++}$ and $^3He^4He^{++}$ listed in Table 5.1. of Appendix A have also reached an accuracy of less than 1%, compared to the most accurate data [48].

4. Conclusions

In conclusion, we have accomplished the goal of this Letter, successfully constructing a generalized interatomic pair-potential function that is able to describe accurately and adequately the potentials for a range of diatomic systems. Very recently, Marques et al. [50] have implemented Rydberg-London potential [19] in their simulation software and demonstrated that Rydberg-London potential is more reliable than the Lennard-Jones potential [23] to be used as starting geometries to obtain global minima of atom clusters. Given that our newly constructed potential has been demonstrated to be more accurate than Rydberg-London potential (see the detailed comparisons between two potential functions for Ar_2, Kr_2, NO, OH, N_2, Li_2, and H_2 presented in Appendix A), it would be interesting and worthwhile to re-examine the consequences of these differences in Monte Carlo searches for low-energy states of atom clusters and bio-molecules [4,50], in numerical simulations [3] of phase transitions and reactions far from equilibrium, and in other large-scale simulation or modeling [4,5] by using our interatomic pair-potential function as the two-body term in a many-body expansion of the interatomic potentials of the system.

We would like to thank Roland E. Allen, Klaus Franzreb, Bo Gao, Jiangbin Gong, Michael C. Heaven, Paul L. Houston, Paul S. Julienne, Robert J. Le Roy, Fuli Li, Steve Scheiner, and Eite Tiesinga for helpful discussions and constructive suggestions.

Appendix A. Supplementary data

Supplementary (In this supporting material, we provide all case studies that we have demonstrated, and a Nonlinear Least Square Fortran (Fortran 90) program and input/output files for H_2 and Ar_2.) data associated with this article can be found, in the online version, at http://dx.doi.org/10.1016/j.cplett.2014.05.021.

References

[1] J. Goodisman, Diatomic Interaction Potential Theory: vol. 1: Fundamentals, and, vol. 2: Applications., Academic Press, New York, 1973.
[2] I.G. Kaplan, Intermolecular Interactions: Physical Picture, Computational Methods, and Model Potentials, John Wiley & Sons, New Jersey, 2006.
[3] M.P. Allen, D.J. Tildesley, Computer Simulation of Liquids, Clarendon Press, Oxford, 1991.
[4] A.R. Leach, Molecular Modelling: Principles and Applications, Pearson Education, New Delhi, 2003.
[5] M. Finnis, Interatomic Forces in Condensed Matter, Oxford University Press, Oxford, 2010.
[6] V. Brites, K. Franzreb, J.N. Harvey, S.G. Sayres, M.W. Ross, D.E. Blumling, A.W. Castleman Jr., M. Hochlaf, Phys. Chem. Chem. Phys. 13 (2011) 15233.
[7] J.S. Winn, Acc. Chem. Res. 14 (1981) 341.
[8] J. Banerjee, D. Rahmlow, R. Carollo, M. Bellos, E.E. Eyler, P.L. Gould, W.C. Stwalley, J. Chem. Phys. 138 (2013) 164302.
[9] R.H. Xie, J.B. Gong, Phys. Rev. Lett. 95 (2005) 263202.
[10] R.H. Xie, P.S. Hsu, Phys. Rev. Lett. 96 (2006) 243201.
[11] J.C. Xie, T. Kar, R.H. Xie, Chem. Phys. Lett. 591 (2014) 69.
[12] K.T. Tang, J.P. Toennies, J. Chem. Phys. 80 (1984) 3726.
[13] G. York, R. Scheps, A. Gallagher, J. Chem. Phys. 63 (1975) 1052.
[14] M. Born, J.E. Mayer, Z. Phys. 75 (1932) 1.
[15] J.C. Xie, T. Kar, S.K. Mishra, R.H. Xie, Chem. Phys. Lett. 593 (2014) 77.
[16] J. Cizek, J. Chem. Phys. 45 (1966) 4256.
[17] Gaussian 09, Revision D.01, M.J. Frisch, et al., Gaussian Inc, Wallingford, CT, 2009.
[18] W. Kolos, J. Rychlewski, J. Chem. Phys. 98 (1993) 3960 (and related references therein).
[19] K. Cahill, V.A. Parsegian, J. Chem. Phys. 121 (2004) 10839.
[20] P.M. Morse, Phys. Rev. 34 (1929) 57.
[21] Y.P. Varshni, Rev. Mod. Phys. 29 (1957) 664.
[22] H.M. Hulbert, J.O. Hirschfelder, J. Chem. Phys. 35 (1961) 1901.
[23] J.E. Lennard-Jones, Proc. Roy Soc. (London) A 106 (1924) 463.
[24] R. Rydberg, Z. Phys. 73 (1932) 376.
[25] O. Klein, Z. Phys. 76 (1932) 226.
[26] A.L.G. Rees, Proc. Phys. Soc. London 59 (1947) 998.
[27] I. Tobias, J.T. Vanderslice, J. Chem. Phys. 35 (1961) 1852.
[28] L. Wolniewicz, J. Chem. Phys. 43 (1965) 1087.
[29] W. Kolos, J.M. Peek, Chem. Phys. 12 (1976) 381.
[30] M. Stanke, D. Kedziera, M. Molski, S. Bubin, M. Barysz, L. Adamowicz, Phys. Rev. Lett. 96 (2006) 233002.
[31] K. Pachucki, Phys. Rev. A 85 (2012) 042511.
[32] W. Kolos, Int. J. Quantum Chem. 10 (1976) 217.
[33] W.C. Tung, M.P. Pavanello, L. Adamowicz, J. Chem. Phys. 137 (2012) 164305.
[34] R.S. Ram, M. Dulick, B. Guo, K.-Q. Zhang, P.F. Bernath, J. Mol. Spectrosc. 183 (1997) 360.
[35] B. Fernandez, H. Koch, J. Chem. Phys. 109 (1998) 10255.
[36] R.A. Aziz, J. Chem. Phys. 99 (1993) 4518.
[37] K.T. Tang, J.P. Toennies, J. Chem. Phys. 118 (2003) 4976.
[38] D.R. Lide, H.V. Kehiaian, CRC Handbook of Thermophysical and Thermochemical Data, CRC Press, Boca Raton, 1994. pp. 69–71.
[39] W.J. Balfour, A.E. Douglas, Can. J. Phys. 48 (1970) 901.
[40] C.R. Vidal, H. Scheingraber, J. Mol. Spectrosc. 65 (1977) 46.
[41] H. Knöckel, S. Rühmann, E. Tiemann, J. Chem. Phys. 138 (2013) 094303.
[42] P. Li, W. Xie, K.T. Tang, J. Chem. Phys. 133 (2010) 084308.
[43] E. Tiesinga, S. Kotochigova, P.S. Julienne, Phys. Rev. A 65 (2002) 042722.
[44] L. Pauling, J. Chem. Phys. 1 (1933) 56.

[45] H. Yagisawa, H. Sato, T. Watanabe, Phys. Rev. A 16 (1977) 1352.
[46] A. Metropoulos, C.A. Nicolaides, R.J. Buenker, Chem. Phys. 114 (1987) 1.
[47] J. Ackermann, H. Hogreve, J. Phys. B 25 (1992) 4069.
[48] L. Wolniewicz, J. Phys. B 32 (1999) 2257.
[49] M. Guilhaus, A.G. Brenton, J.H. Beynon, M. Rabrebovic, P. von Rague? Schleyer, J. Phys. B 17 (1984) L605.
[50] J.M.C. Marques, F.B. Pereira, J. Comput. Chem. 34 (2013) 505. and references therein.